Mineralogy and Petrology (2006) 88: 419–441
DOI 10.1007/s00710-006-0121-0

Mineralogy and Petrology

Printed in Austria

The lithosphere beneath the Sangilen Plateau, Siberia: evidence from peridotite, pyroxenite and gabbro xenoliths from alkaline basalts

V. V. Egorova, N. I. Volkova, R. A. Shelepaev, and **A. E. Izokh**

Institute of Geology and Mineralogy, Russian Academy of Sciences, Novosibirsk, Russia

Received October 29, 2005; revised version accepted February 8, 2006
Published online July 20, 2006;
Editorial handling: S. Maaloe

Summary

Ultramafic and mafic xenoliths in Ordovician Agardag alkaline basalt dikes from the Sangilen Plateau, southeastern Siberia, provide samples from the upper mantle and crust beneath central Asia. Three major groups were distinguished among the xenoliths: Group I xenoliths are spinel lherzolites, Group II xenoliths are spinel-garnet clinopyroxenites, and Group III comprises gabbroic xenoliths with two subgroups: Group IIIa comprises garnet bearing gabbroids and Group IIIb is represented by garnet-free gabbroids. The spinel lherzolite xenoliths represent the uppermost lithospheric mantle beneath the Sangilen Plateau and have geochemical characteristics similar to those of primitive mantle. Spinel-garnet clinopyroxenite and gabbroic xenoliths are of igneous origin and represent fragments of intrusive bodies crystallized at depths close to the mantle-crust boundary, as well as in the lower and the upper crust. The gabbroic xenoliths are evidently the crystallization products of melts similar in major and trace element composition to parental magma of the Bashkymugur gabbronorite-monzodiorite intrusion. Gabbroic xenoliths from the Ordovician Agardag alkaline basalt dikes demonstrate the presence of intermediate magmatic chambers within the crust beneath the Sangilen Plateau during the Early Palaeozoic. The relatively high equilibration temperatures of the mantle and lower crust xenoliths in the Agardag alkaline basalt dikes are largely attributable to a plume occurring beneath the Sangilen Plateau during the Ordovician.

Introduction

Ultramafic and mafic xenoliths in continental alkaline basalts and kimberlites provide unique information on the composition, structure and evolution of the upper mantle and lower crust. Moreover, xenoliths formed by cumulate

processes in magma chambers in different depth levels can provide information about the origin and evolution of the melts from which they have precipitated.

A large diversity and abundance of xenoliths is characteristic for many classic xenolith localities, e.g. French Massif Central (*Downes* and *Dupuy*, 1987; *Downes*, 1993), Baltic Shield (*Kempton* et al., 1995), Eifel, Germany (*Loock* et al., 1990), and eastern Australia (*O'Reilly* et al., 1990). In central Asia petrological and geochemical investigations of mantle and lower crust xenoliths have been carried out for central and southeastern Mongolia (*Stosch* et al., 1995, *Ionov* et al., 1998) and eastern Siberia (Baikal rift area) (*Litasov* et al., 2000). These studies have been carried out on xenoliths from Tertiary or Quaternary magmatic hosts. In contrast, studies of xenoliths entrained by Palaeozoic basalts, are less common and as a consequence, much less is known about the upper mantle and the lower crust sampled by these basalts. We have studied mantle and crustal xenoliths from Ordovician alkaline basalts of the Sangilen Plateau (South Siberia) which provide an exceptional opportunity to investigate the composition and structure of the upper mantle and the crust beneath Central Asia during the Early Palaeozoic.

Usually, lower crustal xenoliths are considered to be metamagmatic rocks re-equilibrated under granulite facies conditions (*Kempton* et al., 2001; *Loock* et al., 1990; *Rudnick* and *Jackson*, 1995). However, mafic xenoliths from alkaline basalts of the Sangilen Plateau are represented by gabbroids with cumulative textures without any features of recrystallization, which are high pressure analogues of Ordovician gabbro-monzodiorite intrusions of the Sangilen Plateau. The interest in gabbroic xenolith from alkaline basalts lies in their evidence for the presence of intermediate magma chambers at the crust-mantle boundary and within the crust beneath the Sangilen Plateau. They are thus important to our understanding of magmatic processes that occurred at different depths of the Central Asian crust during Early Paleozoic times.

The purpose of this paper is to present the results of our detailed study on mineralogy and petrology of peridotitic xenoliths, which supposedly represent the upper mantle beneath the Sangilen Plateau, Central Asia, as well as pyroxenitic and gabbroic xenoliths, which are crystallization products of basaltic melts under various crustal P–T conditions.

Geological setting and host rocks

The Central Asian Orogenic Belt (CAOB) is a complex collage of island arcs, continental blocks and fragments of oceanic crust that accreted to the Siberian Craton during the Neoproterozoic to Palaeozoic (Fig. 1A). One of the large continental blocks within the CAOB is the Tuva-Mongolian Microcontinent. The Sangilen Plateau marks the south-western border of the Tuva-Mongolian Microcontinent and consists of several intrusive and metamorphic complexes. All complexes belonging to the Sangilen Plateau were traditionally regarded as Precambrian basement of the Tuva-Mongolian Microcontinent, comprising Palaeoproterozoic and Archaean rocks (*Ilyin*, 1990; *Zonenshain* et al., 1990). However, recent geochronological studies yielded predominantly Early Palaeozoic ages for

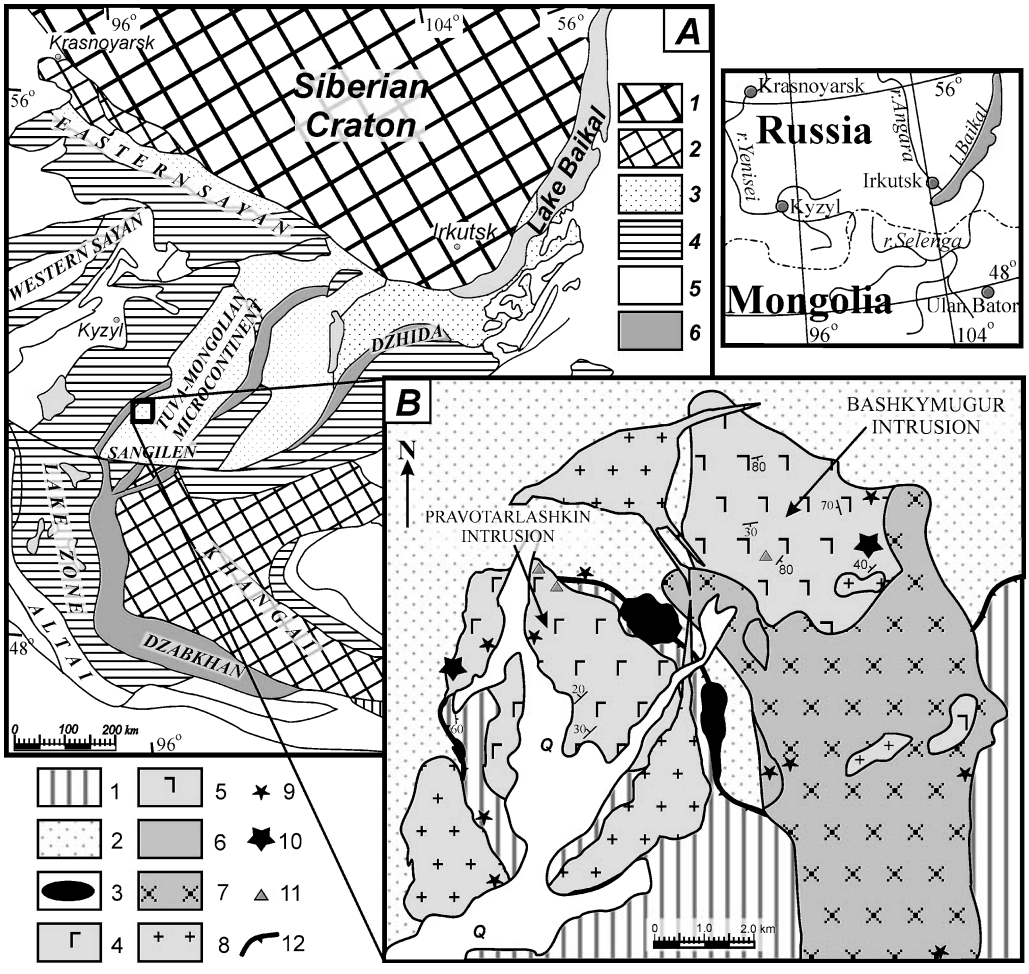

Fig. 1. **A** – Simplified tectonic scheme of the central part of the Central Asian Orogenic Belt (after *Vladimirov* et al., 1999). 1 – Siberian craton; 2 – Precambrian microcontinental megablock; 3 – Riphean microcontinental blocks; 4 – Neoproterozoic mobile belts; 5 – Paleozoic mobile belts; 6 – ophiolites. **B** – Location map of the Agardag alkaline basalt dikes of the Sangilen Plateau. 1 – Precambrian terrigenous – carbonaceous metamorphic rocks of the Moren complex, 2 – Cambrian volcanogenic – sedimentary rocks; 3 – serpentinites; 4 – gabbroids of the Pravotarlashkin intrusion (troctolites, anorthosites, gabbro, gabbronorites); 5–7 – Bashkymugur intrusion: 5 – gabbroids (pyroxenites, gabbronorites, anorthosites and monzogabbros), 6–7 – monzodiorites; 6 – porphyritic; 7 – non-porphyritic; 8 – Ordovician granites; 9–11 – Ordovician Agardag alkaline basalt dikes; 9 – with megacrysts only; 10 – with megacrysts and ultramafic and mafic xenoliths; 11 – mingling dykes with syenites; 12 – faults

the metamorphic rocks and intrusive complexes of the Sangilen Plateau (*Salnikova* et al., 2001; *Izokh* et al., 2001).

At present the Sangilen Plateau is considered to be a complex folded structure, composed of separate sheets, represented by the Moren, Erzin, and Naryn metamorphic complexes. The Moren Complex consists of metatonalites, kyanite-bearing gneisses, migmatites, amphibolites, marbles, quartzites and minor ultra-

mafic lenses. The Erzin Complex is composed of garnet-bearing gneisses, migmatites, granulites and metavolcanic rocks (tholeiites, andesites, dacites). The Naryn Complex includes low-grade metapelites and calcareous quartzites.

These metamorphic complexes are intruded by Early Palaeozoic intrusions of ultramafic to acidic compositions. Among the magmatic rocks, granitoids of different composition and geological setting are widespread. *Kozakov* et al. (1999) published U–Pb ages obtained from zircons, which indicate granite formation in the Sangilen Plateau at 530 to 460 Ma. A wide development of high-grade metamorphic complexes, as well as basic and granitoid magmatism in the CAOB is considered to be a result of a plume activity during the Early Palaeozoic (*Kovalenko* et al., 2004).

Geochronological studies of basic magmatism revealed four age intervals for its evolution, but all these intervals were related to the Cambrian-Ordovician: the Pravotarlashkin troctolite-anorthosite-gabbro intrusion was dated at 524 ± 9 Ma, the Bashkymugur gabbronorite-monzodiorite intrusion was formed at 465 ± 1.2 Ma, the Bayankol gabbronorite-monzodiorite intrusion was formed at 489 ± 3 Ma, and the Agardag dike complex of alkaline basalts and camptonites (*Izokh* et al., 2001) represents the youngest episode of basic magmatism. They are dated at 447–441 Ma using the Ar–Ar method on megacrysts of phlogopite and amphibole (*Izokh* et al., 2001).

The alkaline basalts are located in the north-western part of the Sangilen Plateau and are predominantly northwest–southeast striking dikes. The dikes extension is rarely more than 100 meters, in some cases up to 1 kilometer, while the dike thickness never exceeds 3–5 meters. Dikes intrude metamorphic rocks of the Moren Complex and Cambrian volcanogenic-sedimentary rocks, as well as the Pravotarlashkin and the Bashkymugur intrusions (Fig. 1B).

Large xenoliths are found only in two dikes. One of them is located in the northern part of the Pravotarlashkin intrusion, and another one cuts the eastern part of the Bashkymugur intrusion at the right bank of Tarlashkin-Khem River (Fig. 1B). The xenoliths in the first dike are less than 12 centimeters in diameter. The xenolith content is 25 vol.%. The second dike contains a large amount of xenoliths (more than 75 vol.%), the size of which reaches up to 50 centimeters. The lithologies of the xenoliths in both the dikes are the same comprising spinel lherzolites, garnet-bearing and garnet-free clinopyroxenites, gabbronorite and gabbro with garnet varieties. There are no granitic and metamorphic xenoliths, although these rocks are widespread near the location of the alkaline basalts.

Analytical methods

Fresh xenoliths were selected for chemical and mineralogical analysis. Major element compositions of minerals were analyzed on a Camebax electron microprobe in the Institute of Geology, Siberian Branch, Russian Academy of Sciences in Novosibirsk. Accelerating voltage was 20 kV, a sample current of 40 nA and a beam diameter of 2–3 μm were used. Natural and synthetic minerals were used as standards, and raw data were corrected online using the PAP correction program.

Whole-rock major elements were determined using the X-ray analyzer VRA-20 R by standard X-ray fluorescence techniques at the Analytical Center of the Institute of

Geology SB RAS, Novosibirsk. Trace elements for 4 lherzolite samples, 1 pyroxenite and 8 gabbro xenoliths were analyzed by ICP-MS using the ''Plasma Quad PQ II Turbo Plus'' mass spectrometer at the Institute of Geochemistry SB RAS, Irkutsk, Russia. Relative errors were 5–10%, the detection limits were 0.1 to 1 ppm for various elements.

Petrography of xenoliths

36 xenoliths from the Agardag alkaline basalts were studied in this work. They are subangular to round in shape and range in size from 2 to 20 centimeters. Three major groups were distinguished based on mineral parageneses: Group I – spinel lherzolite, Group II – spinel-garnet clinopyroxenite, and Group III – gabbroid with two subgroups (IIIa – garnet gabbroids and IIIb – garnet-free gabbroids).

Group I – spinel lherzolite

Spinel lherzolite xenoliths are unusually fresh and are characterized by a four-phase mineral assemblage: olivine, orthopyroxene, clinopyroxene and brown spinel. No hydrous minerals were found. Peridotite textures are largely protogranular. Olivine, clinopyroxene and orthopyroxene occur as equant grains sized from 3 to 5 millimeters. The grains generally have straight or gently curved boundaries and show only little evidence of strain in the form of undulose extinction. Brown spinel is found as weakly elongated euhedral crystals as well as anhedral.

Group II – spinel-garnet clinopyroxenite

Garnet-spinel clinopyroxenite samples contain clinopyroxene, garnet and green spinel with minor amounts of plagioclase up to 3 vol.%. They display cumulate texture. Clinopyroxene occurs as elongate green grains up to 8 millimeters in length. Deep-green spinel forms grains of irregular shape and the spinel modal content reaches 20 vol.%. Garnet occurs usually as euhedral and rounded crystals, or, more rarely, forms chains within the clinopyroxene grains. Garnet grains are replaced by dark kelyphitic rims, identical in bulk chemical composition to the primary garnet. Plagioclase commonly occurs as subhedral to xenomorphic interstitial grains between clinopyroxene grains.

Group III – gabbroid xenoliths

These xenoliths consist mainly of variable amounts of clinopyroxene, orthopyroxene, plagioclase and amphibole (gabbronorite and gabbro). This group is subdivided into two subgroups: garnet-bearing (Group IIIa) and garnet-free (Group IIIb) gabbroids. Both subgroups are characterized by massive or banded textures, showing alternation of plagioclase-rich and pyroxene-rich layers 2–3 centimeters wide, as well as gabbroic and gabbro-ophitic textures. Grain size of the minerals is less than 5 millimeters. Clinopyroxene forms brown–green unzoned euhedral, slightly elongated, grains and often includes small sulfide globules. Orthopyroxene displays strong pleochroism from deep rose to light green. Plagioclase occurs as slightly

elongated subhedral grains, displaying weak zoning. Garnet forms subhedral to euhedral grains, which are commonly surrounded by a brown cryptocrystalline kelyphite aggregate. Kelyphitisation is commonly attributed to heating, either during transport in the host magma or in a lower crustal heating event (*Stosch* et al., 1995) or decompression (*Rudnick* and *Jackson*, 1995). The modal content of magmatic brown amphibole reaches 20 vol.%. Amphibole occurs in xenoliths as anhedral grains, filling interstices between the other minerals and forming replacement rims around clinopyroxene crystals. Accessory minerals are magnetite, titanomagnetite, apatite, ilmenite, titanite and pyrite. Biotite appears as tiny flakes and its amount is usually less than 1–2 vol.%. Cumulate textures without any features of recrystallization suggest the magmatic nature of the gabbroic xenoliths. These xenoliths are similar in texture and mineral composition to rocks of the Bashkymugur intrusion.

Mineral chemistry

Olivine occurs only in the Group I xenoliths. Its Mg number (Mg#) is usually 90 to 89, and NiO content reaches 0.4 wt.%. Only a single sample shows lower Mg# = 86 (Table 1). The CaO content is rather low: 0.06 to 0.12 wt.%.

Clinopyroxenes from the Group I spinel lherzolites are aluminian chromian augites according to the pyroxene nomenclature (*Morimoto*, 1988) (Fig. 2A, Table 1). They are characterized by high Mg numbers (Mg# = 85–90), high Cr_2O_3 (0.9–1.4 wt.%) and TiO_2 (0.3–0.7 wt.%) contents. Al_2O_3 and Na_2O contents vary from 5.8 to 7.3 wt.% and 1.2 to 1.9 wt.%, respectively.

Clinopyroxenes from spinel-garnet clinopyroxenites (Group II) are aluminian diopsides (*Morimoto*, 1988) with Mg# = 87–89 (Fig. 2A, Table 1). They contain more Al_2O_3 (9–11.5 wt.%) compared to clinopyroxenes of Group I, but have lower contents of sodium, titanium and chromium (Na_2O = 1–1.3 wt.%, TiO_2 = 0–0.23 wt.%, Cr_2O_3 = 0.15–0.30 wt.%).

Clinopyroxenes of the two gabbroid subgroups are aluminian augites and aluminian diopsides (*Morimoto*, 1988) (Fig. 2A, Table 1). They are characterized by low chromium contents (0.03–0.22 wt.%), which are common for lower crust xenoliths (*Rudnick*, 1992). The Group IIIa clinopyroxenes associated with garnet have Mg# 57 to 80 relatively high contents of Al_2O_3 (5.1–8.4 wt.%) and Na_2O (0.7–1.28 wt.%). Clinopyroxenes whose Al-content is highest are also Na-rich (Fig. 3).

Clinopyroxenes in garnet-free samples (Group IIIb) are subdivided into two varieties: with high Al_2O_3 (6.5–7.8 wt.%) and Na_2O (0.7–1.3 wt.%) contents, and with low contents of Al_2O_3 (1.6–3.5 wt.%) and Na_2O (0.35–0.55 wt.%) (Fig. 3). The Mg# of the Group IIIb clinopyroxenes greatly varies from 62 to 80 in high-Al clinopyroxenes and from 56 to 76 in low-Al ones. The Mg# of the clinopyroxenes correlates positively with those of the whole rock compositions of the xenoliths and with Mg# of garnet. The low-Al clinopyroxenes from Group IIIb gabbroic xenoliths fall within the compositional field of clinopyroxenes from the Bashkymugur intrusion (Fig. 3).

Orthopyroxene from spinel lherzolite are chromian enstatite, which have high Mg# of 86–90 and Al_2O_3 contents of 3.9–5.3 wt.%. The Cr_2O_3 content varies from 0.35 to 0.61 wt.% (Fig. 2A, Table 1). Orthopyroxenes from gabbroid xenoliths

Table 1. *Representative chemical compositions of minerals from xenoliths of the Sangilen Plateau*

Sample	I-39 (I)				I-40 (I)				439 (I)				X34 (I)			
(Group) Association	Ol	Cpx	Opx	Spl	Ol	Cpx	Opx	Spl	Ol	Cpx	Opx	Spl	Ol	Cpx	Opx	Spl
SiO_2	40.34	51.64	54.62	0.87	41.15	51.42	54.24	0.05	40.68	52.01	54.34	0.04	41.03	51.64	54.87	0.04
TiO_2	n.d.	0.63	0.22	0.84	n.d.	0.58	0.12	0.16	n.d.	0.29	0.08	0.09	n.d.	0.50	0.16	0.10
Al_2O_3	n.d.	5.78	3.88	36.69	n.d.	7.32	5.26	57.15	n.d.	6.41	5.01	53.87	0.02	5.93	4.66	53.98
Cr_2O_3	0.02	1.33	0.61	24.28	0.02	0.85	0.35	8.71	0.04	0.97	0.54	13.53	0.04	1.02	0.62	13.72
FeO	14.38	4.70	8.79	20.74	10.81	3.56	6.75	11.69	9.51	3.24	6.21	11.57	11.75	3.81	7.13	11.53
MnO	0.25	0.15	0.26	0.22	0.10	0.10	0.16	0.11	0.13	0.06	0.09	0.09	0.18	0.08	0.16	0.07
MgO	45.01	14.82	30.09	14.32	47.79	15.12	31.67	20.65	49.28	15.89	32.36	20.26	47.35	16.38	31.32	20.30
CaO	0.12	18.83	1.09	n.d.	0.05	19.2	0.83	n.d.	0.08	19.48	0.98	n.d.	0.10	19.89	1.08	n.d.
Na_2O	n.d.	1.97	0.21	n.d.	n.d.	1.74	0.13	n.d.	n.d.	1.52	0.16	n.d.	0.03	1.18	0.15	0.02
NiO	0.38	n.d.	n.d.	n.d.	0.35	n.d.	n.d.	n.d.	0.40	n.d.	n.d.	0.32	n.d.	n.d.	n.d.	n.d.
Total	100.2	99.8	99.8	98.0	99.9	99.9	99.5	98.6	100.2	99.9	99.8	99.7	100.5	100.4	100.1	100.1
Mg#	86	91	86	55	89	88	89	77	90	93	92	76	89	88	89	76
Sample	145 (II)				I-35 (II)				KB2 (IIIa)				T6 (IIIa)			
(Group) Association	Cpx	Grt	Kel	Pl	Cpx	Grt	Spl	Pl	Cpx	Opx	Grt	Pl	Cpx	Opx	Grt	Pl
SiO_2	50.24	42.46	42.06	54.76	48.90	42.01	0.01	51.54	48.85	49.13	38.83	52.80	49.28	50.74	39.93	50.05
TiO_2	0.23	0.06	0.06	n.d.	0.01	n.d.	n.d.	n.d.	1.10	0.11	0.15	n.d.	0.50	0.05	0.10	n.d.
Al_2O_3	9.01	23.31	23.20	27.56	11.53	23.58	67.45	31.01	6.89	5.37	21.72	29.55	6.30	4.82	21.82	3.55
Cr_2O_3	0.30	0.16	0.19	n.d.	0.15	0.17	1.72	n.d.	0.04	0.02	0.03	n.d.	0.05	0.03	0.07	n.d.
FeO	3.85	9.66	9.24	0.13	3.23	8.10	10.08	0.08	8.58	22.83	21.84	0.20	8.88	18.93	19.45	0.22
MnO	0.06	0.18	0.21	n.d.	0.08	0.22	0.06	n.d.	0.10	0.22	0.57	n.d.	0.14	0.23	0.60	n.d.
MgO	14.68	18.87	18.91	0.07	13.91	19.02	21.10	0.10	12.18	21.65	11.18	n.d.	12.76	23.91	12.11	n.d.
CaO	19.66	5.14	5.46	10.65	20.82	6.28	n.d.	13.71	20.64	0.78	5.80	12.23	20.54	0.79	5.92	14.63
Na_2O	1.30	0.24	0.38	5.46	1.02	0.05	n.d.	3.87	0.90	0.09	0.05	4.40	0.77	0.05	0.03	3.07
K_2O	n.d.	n.d.	n.d.	0.27	n.d.	n.d.	n.d.	n.d.	n.d.	n.d.	n.d.	0.12	n.d.	n.d.	n.d.	0.12
Total	99.3	100.1	99.7	98.8	99.7	99.4	100.5	100.4	99.3	100.2	100.2	99.4	99.2	99.6	100.0	99.7
Mg#	87	78	78	–	89	81	79	–	72	63	48	–	72	69	53	–

(*continued*)

Table 1 (*continued*)

Sample (Group)	N5g (IIIa)			T2 (IIIa)				T5 (IIIb)			KB3 (IIIb)			
Association	Cpx	Grt	Pl	Cpx	Opx	Grt	Pl	Cpx	Pl	Am	Cpx	Opx	Pl	Am
SiO_2	48.69	37.92	55.25	50.11	52.52	40.92	49.43	50.16	47.86	42.12	49.16	49.57	56.96	39.16
TiO_2	0.65	0.08	n.d.	0.37	n.d.	0.04	n.d.	0.49	n.d.	1.18	0.37	0.03	n.d.	2.34
Al_2O_3	5.11	21.28	28.32	8.43	5.47	22.90	32.58	7.75	33.69	15.45	6.52	4.15	26.58	14.38
Cr_2O_3	0.03	0.07	n.d.	0.08	n.d.	0.03	n.d.	0.09	n.d.	0.14	n.d.	n.d.	n.d.	0.18
FeO	13.77	24.92	0.05	6.26	14.11	16.01	0.09	6.10	0.12	8.39	12.14	25.51	0.16	16.46
MnO	0.31	1.38	n.d.	0.14	0.16	0.49	n.d.	0.19	n.d.	0.11	n.d.	n.d.	n.d.	n.d
MgO	10.13	6.65	n.d.	12.99	26.38	13.94	n.d.	13.57	n.d.	15.00	11.28	20.26	n.d.	10.87
CaO	19.29	7.23	10.57	20.81	0.70	5.94	15.77	21.46	16.90	11.25	18.82	0.85	8.77	9.84
Na_2O	0.75	0.02	5.42	0.99	0.03	0.02	2.61	0.72	1.88	2.55	1.29	0.05	6.68	3.26
K_2O	n.d.	n.d.	0.30	n.d.	n.d.	n.d.	0.06	n.d.	0.05	0.85	n.d.	n.d.	0.15	0.43
Total	98.7	99.5	100.0	100.2	99.4	100.3	100.6	100.5	100.5	97.0	99.6	100.4	99.3	96.9
Mg#	57	32	–	80	77	61	–	80	–	76	62	59	–	54
Sample (Group)	KB6 (IIIb)			KB1 (IIIb)				KB8 (IIIb)			KC17 (IIIb)			
Association	Cpx	Opx	Pl	Cpx	Opx	Pl	Am	Cpx	Opx	Pl	Cpx	Opx	Pl	Am
SiO_2	49.81	51.71	50.63	51.54	53.29	52.00	41.28	51.48	52.62	49.17	51.26	51.41	56.51	41.71
TiO_2	0.16	0.04	n.d.	0.55	0.23	n.d.	3.37	0.42	0.26	n.d.	0.39	0.14	n.d.	3.28
Al_2O_3	7.46	4.25	31.43	2.84	1.61	30.34	12.75	3.25	1.82	32.33	1.62	0.95	27.22	13.49
Cr_2O_3	n.d.	0.06	n.d.	0.04	n.d.	n.d.	0.04	0.10	0.05	n.d.	n.d.	n.d.	n.d.	0.08
FeO	7.91	19.61	n.d.	8.31	17.57	0.23	12.01	8.82	17.68	0.12	11.77	24.23	0.27	12.68
MnO	n.d.	0.53	0.13	n.d.	n.d.	n.d.	n.d.	n.d.	0.34	n.d.	n.d.	n.d.	n.d.	0.19
MgO	12.71	22.63	0.04	14.79	25.47	n.d.	12.91	15.34	24.96	n.d.	13.36	20.33	n.d.	11.94
CaO	21.01	0.84	14.26	21.18	1.00	13.08	11.77	19.75	1.97	15.27	0.99	0.95	9.88	10.97
Na_2O	0.80	0.08	3.29	0.41	n.d.	4.14	2.07	0.39	n.d.	2.62	0.35	n.d.	5.75	2.45
K_2O	n.d.	n.d.	0.19	n.d.	n.d.	0.18	1.49	n.d.	0.06	0.11	n.d.	n.d.	0.28	1.35
Total	99.8	98.8	99.7	99.7	99.2	100.0	97.7	99.5	99.8	99.7	99.8	98.0	100.0	98.14
Mg#	74	67	–	76	72	–	66	76	72	–	67	60	–	62

Note: All Fe as FeO; *Mg#* $Mg^*100/(Mg + Fe_{tot})$ (at.%). *Cpx* clinopyroxene; *Opx* orthopyroxene; *Ol* olivine; *Pl* plagioclase; *Am* amphibole; *Grt* garnet; *Spl* spinel; *Kel* kelyphite; *n.d.* not determined

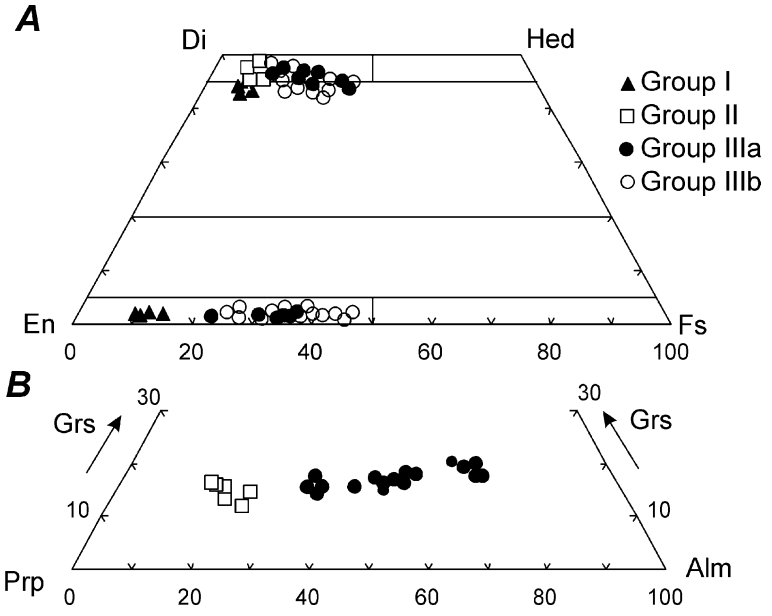

Fig. 2. Compositional range of pyroxenes (A) and garnets (B) from the xenoliths of the Sangilen Plateau

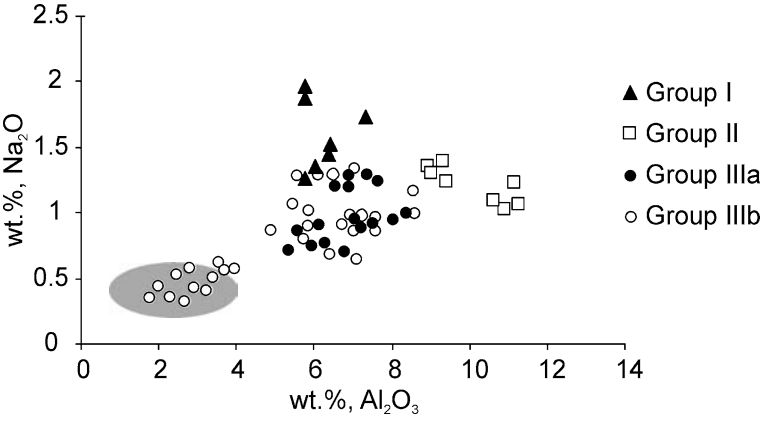

Fig. 3. Diagram Al_2O_3 and Na_2O contents of clinopyroxenes from the xenoliths of the Sangilen Plateau. Gray field: clinopyroxenes from rocks of the Bushkymugur intrusion

correspond in composition to enstatite with a Mg# of 63 to 77 in Group IIIa and 55 to 72 in Group IIIb. Like clinopyroxenes, the Group IIIb orthopyroxenes are subdivided into two varieties according to their alumina content: (a) high-Al (4.3 to 5.2 wt.% of Al_2O_3), (b) and low-Al (0.9 to 1.8 wt.% of Al_2O_3). High-Al orthopyroxenes are associated with high-Al clinopyroxenes. The Group IIIb low-Al orthopyroxenes show similar chemical compositions with orthopyroxenes of Bashkymugur intrusion.

Garnet from the garnet clinopyroxenites is rich in pyrope and almandine end-members ($Prp_{62–69}$, $Alm_{16–23}$, $Grs_{13–16}$), Mg# = 78–81, with no compositional

zoning (Fig. 2B, Table 1). Garnet grains are replaced by dark kelyphitic rims, with an identical bulk chemical composition to the primary garnet. Garnet from the gabbroid xenoliths of Group IIIa is also unzoned pyrope-almandine (Prp_{25-52}, Alm_{33-54}, Grs_{15-20}), but its Mg# is lower ranging from 32 to 61. The CaO content reaches up to 7 wt.% (Table 1). Kelyphitic rims correspond in composition to garnet; only some analyses display high contents of Na_2O up to 3.4 wt.%. The Mg# of garnet increases with increasing Mg# of coexisting pyroxenes.

Plagioclase from the spinel-garnet clinopyroxenite (Group II) are generally labradorite (An_{52-66}) (Table 1). Gabbroid xenoliths plagioclases vary from labradorite-bytownite (An_{60-83}) to andesine (An_{47-49}). Grains are generally homogeneous; however, minor normal zoning (2–7 mol% An) was detected in a few samples. The Mg# of coexisting pyroxenes decreases regularly with a decrease of the anorthite content in plagioclases in Groups IIIa and IIIb. The low magnesian pyroxenes coexist with andesine, while high magnesian pyroxenes coexist with labradorite-bitownite. This is a specific feature of fractional crystallization of a basalt melt in a magmat chamber.

Amphiboles from xenoliths of Group III range from titanian magnesio-hastingsite to pargasite (*Leake* et al., 1997) (Table 1). Their Mg# ranges from 54 to 76. The titanium content varies from 0.18 to 3.37 wt.%, garnet-bearing samples contain 1.25 to 2 wt.% of TiO_2.

Spinel in the Group I xenoliths is a brown Cr-spinel with Mg# = 55–76, and Cr# = 9–31 (Table 1). Its NiO content is 0.32 to 0.35 wt.%. Spinel-garnet clinopyroxenites contain green Cr-free Al-rich spinel (Cr# < 5) with Mg# = 69–79. It has lower contents of NiO (0.15–0.21 wt.%). Sometimes, a green Cr-free Al-rich spinel, but with lower Mg-number (Mg# = 58) is present in the gabbroid xenoliths, as well as in the Group II xenoliths.

Equilibrium pressure and temperature

Several geothermobarometers were used to estimate equilibrium *T–P* conditions of the Sangilen Plateau xenoliths. The pyroxene geothermometers of *Brey* and *Köhler* (1990) is commonly used for temperature estimates of mantle xenoliths. Temperatures obtained from the spinel lherzolites range from 1028 to 1124 °C using the two-pyroxene thermometer and from 1020 to 1100 °C using the Ca in orthopyroxene thermometer (*Brey* and *Köhler*, 1990). Calculated pressures are from 18 to 23 kbar (Cr in spinel barometer; *Webb* and *Wood*, 1986) and from 19 to 21 kbar (clinopyroxene barometer; *Mercier*, 1980). The results are close to the depth of the transition from spinel to garnet lherzolites. The garnet-spinel clinopyroxenites equilibrated over a pressure range of 12.7 to 14.2 kbar (*Mercier*, 1980) or 9.7 to 10.6 kbar (Grt-Pl-Cpx barometer; *Newton* and *Perkins*, 1982) and a temperature range from 930 to 1010 °C from the Grt-Cpx thermometer (*Powell*, 1985) (Table 2). These calculated *P–T* conditions imply that the xenoliths are derived from both the lower crust and the uppermost mantle.

The presence of aluminous pyroxenes in the gabbroid xenoliths is consistent with a high pressure origin. The presence of pyrope-almandine garnet in the Group IIIa xenoliths suggests a pressure of more than 12–14 kbar at 900–1050 °C (*Irving*, 1974; *Gasparik*, 1984). The estimates of temperatures and pressures for the

Table 2. *P–T calculations for xenoliths of the Sangilen Plateau*

Sample (Group)	T, °C					P, kbar						
	1	2	3	4	5	6	7	8	9	10	11	12
439 (I)	1073	1056	–	–	–	19.0	19.5	–	–	–	–	–
I-39 (I)	1124	1100	–	–	–	21.1	23.2	–	–	–	–	–
I-40 (I)	1028	1020	–	–	–	19.1	18.5	–	–	–	–	–
145 (II)	–	–	1010	1100	–	13.7	–	10.4	–	–	–	–
I-35 (II)	–	–	934	1140	–	12.7	–	9.7	–	–	–	–
T1 (IIIa)	861	–	1040	1048	934	–	–	–	11.0	9.2	–	8.8
T6 (IIIa)	1049	–	1045	1057	983	–	–	–	12.6	10.5	–	8.3
KB2 (IIIa)	1163	–	1066	1075	1013	–	–	–	11.6	12.0	–	–
N5g (IIIa)	–	–	890	910	–	–	–	–	–	–	–	–
T3 (IIIb)	1020	–	–	–	1000	–	–	–	–	–	9.2	9.0
T5 (IIIb)	–	–	–	–	–	–	–	–	–	–	10.4	9.4
KB3 (IIIb)	–	–	–	–	–	–	–	–	–	–	9.5	8.5
KB6 (IIIb)	–	–	–	–	–	–	–	–	–	–	10.6	10.0
KB1 (IIIb)	1023	–	–	–	1041	–	–	–	–	–	5.0	5.5
KB8 (IIIb)	1010	–	–	–	1097	–	–	–	–	–	5.3	6.7
KC17 (IIIb)	1020	–	–	–	1049	–	–	–	–	–	2.5	3.9

Note: Using *thermometers* – 1 – Opx-Cpx, *Brey* and *Kohler*, 1990; 2 – Ca in Opx, *Brey* and *Kohler*, 1990; 3 – Grt-Cpx, *Powell*, 1985; 4 – Grt-Cpx, *Ellis* and *Green*, 1979; 5 – Opx-Cpx, *Sen* and *Jones*, 1989; and *barometers* – 6 – Cpx, *Mercier*, 1980; 7 – Cr in Spl, *Webb* and *Wood*, 1986; 8 – Grt-Pl-Cpx, *Newton* and *Perkins*, 1982; 9 – Grt-Opx, *Harley*, 1984; 10 – Grt-Opx, *Nickel* and *Green*, 1985; 11 – Cpx, *Nimis*, 1999; 12 – Am, *Hammarstrom* and *Zen*, 1986

gabbroid xenoliths group were obtained using the garnet-clinopyroxene (*Powell*, 1985; *Ellis* and *Green*, 1979), and the two-pyroxene (*Sen* and *Jones*, 1989) thermometers and the garnet-orthopyroxene barometers (*Harley*, 1984; *Nickel* and *Green*, 1985). Finally, for amphibole-bearing varieties we used three amphibole barometers (*Hammarstrom* and *Zen*, 1986; *Hollister*, 1987; *Schmidt*, 1991).

The equilibrium temperatures and pressures for xenoliths of Group IIIa were estimated to be 1000–1070 °C (*Powell*, 1985, *Ellis* and *Green*, 1979) and 11–13 kbar (*Harley*, 1984). Two-pyroxene thermometers gave similar results (Table 2). The temperature estimates (940–1000 °C) obtained using the two-pyroxene thermometer are similar for garnet-free varieties and garnet-bearing samples.

The pressure determination for garnet-free varieties (Group IIIb) presents difficulties for lack of any barometers for basic systems, based on equilibrium of garnet-free parageneses. Therefore the pressures were estimated using the amphibole barometers. In addition, for garnet-free xenoliths we used the pyroxene barometer (*Nimis*, 1999), which allows determination of crystallization pressure for magmatic assemblages containing $Cpx \pm Opx \pm Pig \pm Pl \pm Spl \pm Mgt \pm Amp \pm Ilm$, based only on clinopyroxene composition. Group IIIb xenoliths with high-alumina clinopyroxene have equilibrated over a pressure range of 8.5 to 10.6 kbar, based on amphibole barometry, and 8 to 9.8 kbar, based on clinopyroxene barometry. Gabbroid xenoliths with low-alumina clinopyroxene equilibrated at $T = 1000–1100$ °C,

based on the two-pyroxene thermometer, and P = 4–8 kbar from amphibole barometer or P = 3.9–6.7 kbar from pyroxene barometer (Table 2).

Whole rock composition

Major elements

Major and trace element compositions of xenoliths are given in Table 3. Group I xenoliths are ultramafic and are distinguished from the other considered xenoliths by their high MgO contents (>37 wt.%), coupled with low concentration of Al_2O_3 (2.8–3.5 wt.%), CaO (3.1–3.9 wt.%), alkalis ($Na_2O + K_2O = 0.1$–0.14 wt.%) and TiO_2 (0.15 wt.%) Peridotite xenoliths vary in composition from undepleted (low MgO – 37.8–38.9 wt.%, high Al_2O_3, high CaO) to somewhat more depleted (higher MgO – 40.6–41.1 wt.%, lower Al_2O_3 and CaO).

Group II xenoliths are also of ultramafic composition (SiO_2 – 39–46 wt.%), but are characterized by considerably lower MgO contents of 16–19 wt.%, with Mg# = 70–79 and high contents of Al_2O_3 ranging from 14 to 21 wt.% and CaO (10–15 wt.%). The Group II xenoliths low TiO_2 contents with a maximum of 0.15 wt.%, suggest that these rocks are not high-pressure cumulates of alkaline basalt magma.

All Group III xenoliths have mafic compositions, with SiO_2 ranging from 44.5 to 52.5 wt.%. Mg# ranges from 28 to 64 and total alkalis from 2.2 to 5.4 wt.%. They are characterized by moderate MgO contents of 4.8–11.2 wt.% and high Al_2O_3 contetns ranging from 11–23 wt.%. CaO shows a significant variation between values of 8.5 and 18 wt.%. TiO_2 content varies from 0.18 to 2.5 wt.% and along with alkalis shows a fairly well-developed negative correlation with the MgO content (Fig. 4). In this case Ti behaves as incompatible element and along with Na and K accumulates in a melt. The enrichment of the xenoliths in Ti, Na, K suggests fractionation in a magma chamber.

Trace elements

Rare earth element contents in two analyzed spinel lherzolites are low and similar to those estimated for the primitive mantle (*Sun* and *McDonough*, 1989). They are characterized by flat primitive mantle-normalized patterns with slight LREE depletion in sample I-40 (Fig. 5A). La/Yb ratios vary from 0.9 to 1.2.

Group II xenoliths have higher HREE contents than spinel lherzolites (Fig. 5A, Table 3), but are depleted in LREE with $(La/Sm)_n = 0.08$. Garnet pyroxenites display REE patterns typical of these rocks with enrichment in HREE and depletion in LREE, with $(La/Yb)_n$ ratio is 0.02.

Gabbroid rare earth element contents are 2–35 times the primitive mantle values. All the Group III xenoliths have similar LREE-enriched patterns with a $(La/Yb)_n$ ratio ranging from 1.4 to 9. The only difference between samples of this group is the level of total REE content, which increases with decreasing Mg# in both of Group IIIa and Group IIIb xenoliths. This suggests the increase of total REE content during fractional crystallization. Gabbroic xenoliths of Groups IIIa and IIIb have minor positive Eu anomalies ($(Eu/Eu^*)_n = 1.1$–2.5). However, two

Table 3. *Representative major (wt.%) and trace element analyses (ppm) of xenoliths of the Sangilen Plateau*

Sample	I-40	I-39	439	X34	I-35	T1	T6	KB2	KB6	KB1	KB8	KC13	KC17	SH3
Group	I	I	I	I	II	IIIa	IIIa	IIIa	IIIb	IIIb	IIIb	IIIb	IIIb	
SiO_2	44.1	48.2	43.9	43.2	44.0	49.9	46.7	45.9	46.5	48.9	45.8	52.5	48.12	48.3
TiO_2	0.14	0.15	0.07	0.08	b.d.	0.30	0.54	1.18	0.39	0.42	0.38	1.09	1.57	0.50
Al_2O_3	3.53	2.78	3.23	3.15	14.85	19.80	18.83	19.93	19.15	11.63	16.90	17.11	17.64	13.01
Fe_2O_3	8.95	3.97	8.86	8.75	4.99	9.08	9.12	9.98	7.09	5.97	13.57	8.84	12.55	6.93
MnO	0.15	0.17	0.12	0.12	0.16	0.24	0.16	0.16	0.13	0.15	0.22	0.17	0.16	0.22
MgO	37.82	38.93	40.62	41.17	18.94	6.91	9.50	6.87	7.42	11.02	11.28	4.87	4.89	16.18
CaO	3.11	3.89	3.08	3.23	15.34	11.42	12.35	12.30	13.15	17.94	8.71	8.57	9.50	10.16
Na_2O	b.d.	b.d.	0.06	0.10	0.66	2.62	1.70	2.75	3.13	1.83	1.91	4.60	4.14	2.90
K_2O	0.05	0.08	0.04	0.04	0.19	0.03	0.22	0.47	1.04	0.37	0.27	0.78	0.64	0.40
Total	99.0	99.1	99.8	99.9	100.2	100.4	99.3	100.2	100.0	99.5	99.1	99.5	99.9	98.6
Mg#	80	91	84	84	79	46	54	41	51	65	45	36	28	70
Rb	n.d.	n.d.	n.d.	n.d.	n.d.	5.78	7.63	2.87	18.07	9.89	6.29	8.39	10.58	8.83
Ba	n.d.	n.d.	n.d.	n.d.	n.d.	47.3	76.9	88.3	223.9	123.2	103.1	238.3	281.2	132.9
Sr	n.d.	n.d.	n.d.	n.d.	n.d.	324	299	338	543	409	705	597	793	238
Th	n.d.	n.d.	n.d.	n.d.	n.d.	0.69	1.00	0.44	b.d.	0.75	0.23	0.85	b.d.	1.07
Nb	n.d.	n.d.	n.d.	n.d.	n.d.	7.22	5.84	2.95	b.d.	4.47	b.d.	2.46	b.d.	1.01
Ta	n.d.	n.d.	n.d.	n.d.	n.d.	0.75	0.78	b.d.	b.d.	0.32	b.d.	0.18	b.d.	0.03
Zr	n.d.	n.d.	n.d.	n.d.	n.d.	31.86	2.59	32.45	45.78	24.85	136.92	41.93	67.83	37.54
Hf	n.d.	n.d.	n.d.	n.d.	n.d.	0.90	0.29	0.75	1.12	0.81	3.12	0.88	1.88	0.94
Y	n.d.	n.d.	n.d.	n.d.	n.d.	4.31	5.75	8.24	10.14	12.17	4.22	19.22	22.72	11.28
La	0.40	0.57	n.d.	n.d.	0.03	3.66	4.01	5.65	9.38	7.05	4.30	22.30	17.44	7.25
Ce	1.32	1.19	n.d.	n.d.	0.3	7.69	9.27	11.73	24.16	13.85	8.10	46.86	39.48	15.34
Pr	0.34	0.17	n.d.	n.d.	n.d.	1.00	1.42	1.68	3.62	1.94	1.08	6.12	5.83	2.14
Nd	2.3	0.70	n.d.	n.d.	2.50	4.40	5.81	6.89	13.38	7.65	4.20	24.16	25.25	10.28
Sm	0.75	0.25	n.d.	n.d.	2.46	0.98	1.57	1.53	2.73	1.82	0.73	5.22	5.53	2.22
Eu	0.31	0.06	n.d.	n.d.	1.03	0.40	0.60	0.68	0.75	0.80	0.62	1.27	1.98	0.63
Gd	1.11	0.26	n.d.	n.d.	3.05	0.93	1.26	1.47	2.42	2.23	0.81	3.88	4.47	1.99
Tb	0.22	0.09	n.d.	n.d.	0.77	0.12	0.18	0.24	0.33	0.36	0.11	0.59	0.68	0.34
Dy	1.30	0.40	n.d.	n.d.	n.d.	0.81	1.22	1.27	1.53	1.79	0.57	2.73	3.30	1.86
Ho	0.20	n.d.	n.d.	n.d.	n.d.	0.17	0.25	0.27	0.35	0.40	0.13	0.59	0.74	0.39
Er	0.40	0.45	n.d.	n.d.	n.d.	0.56	0.63	0.92	1.15	1.42	0.50	2.21	2.27	1.06
Yb	0.31	0.31	n.d.	n.d.	1.01	0.47	0.56	0.94	0.86	1.14	0.49	1.77	1.82	0.95
Lu	0.03	0.05	n.d.	n.d.	0.14	0.07	0.09	0.13	0.13	0.16	0.05	0.24	0.29	0.14

Note: *n.d.* not determined; *b.d.* below detection limit; *Mg#* $MgO^{*}100/(MgO + Fe_2O_3)$; SH3 for olivine gabbronorite of Bushkymugur intrusion

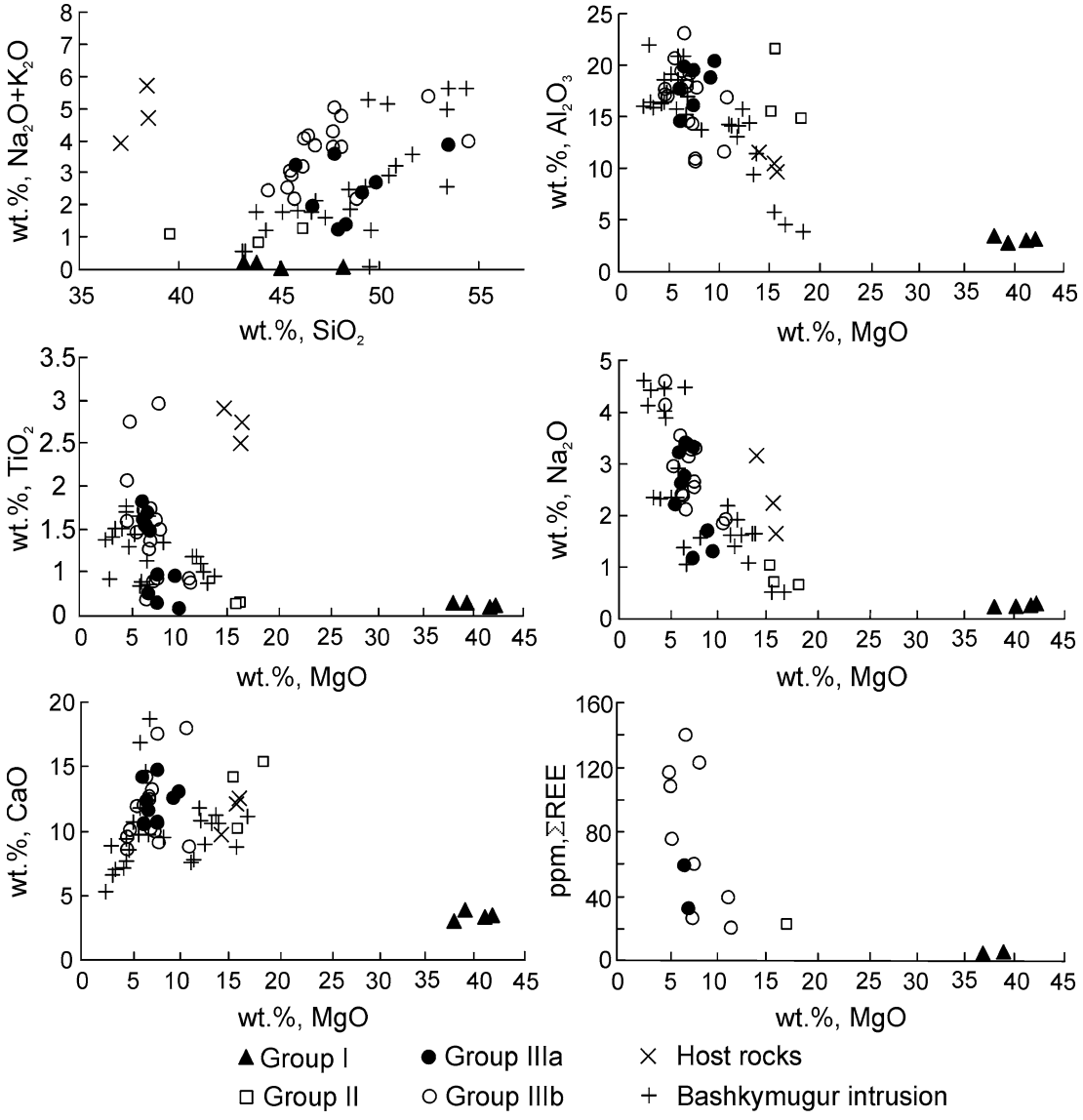

Fig. 4. Major element variation diagrams for xenoliths of the Sangilen Plateau. Data for the rocks of the Bushkymugur intrusion are shown for comparison

Group IIIb xenoliths have a negative Eu anomaly ($(Eu/Eu^*)_n = 0.5–0.86$), despite of their high REE contents and low Mg#.

Most of the gabbroic xenoliths have very similar mantle-normalized trace element patterns characterized by enrichment in LIL elements (Cs, Rb, Ba) and LREE (Fig. 5B). They show characteristic depletion in Nb, Hf, Zr relative to LREEs, Ba, Sr, Rb. Such geochemical features are typical of subduction-related magmatic rocks. The contents of incompatible trace elements such as Sr, Zr and REE increase with decrease in MgO in the gabbroid xenoliths (Fig. 4). This also could reflect melt differentiation in a magma chamber.

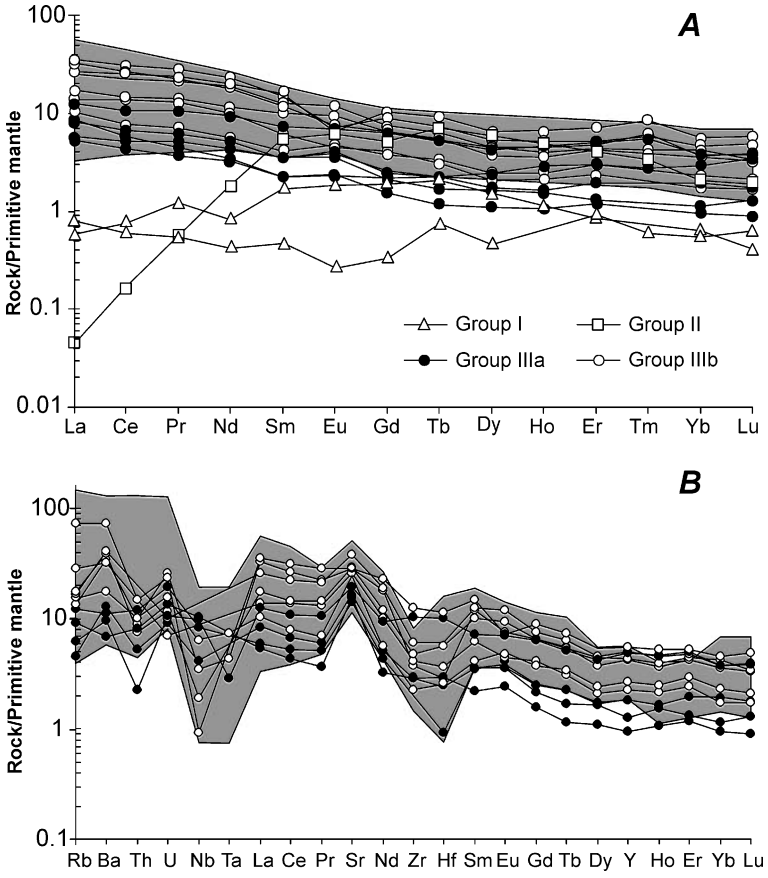

Fig. 5. Primitive mantle-normalized REE patterns (A) and trace elements diagram (B) for the xenoliths of the Sangilen Plateau; the shaded field gives the range of trace element concentrations in rocks of the Bushkymugur intrusion

A comparison of the Group III gabbroid xenoliths with rocks of the Bashkymugur intrusion shows similarities in several major and trace element characteristics (Fig. 5B). They are characterized by negative HFSE anomalies and by enrichment in LILE and Sr. Similar spectra are noted for most of the gabbroid intrusions in the western part of the Sangilen Plateau. The similarity of rock chemical compositions of the Bashkymugur intrusion and gabbroic xenoliths can suggest their genetic relationship, or the resemblance of geochemical types of parental melts for the rocks of both the Bashkymugur gabbronorite-monzodiorite intrusion and gabbroid xenoliths.

Discussion

Origin of xenoliths

Spinel lherzolite xenoliths of the Sangilen Plateau have major element concentrations that fall within the normal variation of mantle-derived spinel peridotites

(*Maaløe* and *Aoki*, 1977; *McDonough*, 1990). Relative to the primitive mantle composition two of the samples are enriched in MgO and depleted in CaO, Al_2O_3 and TiO_2. Two other samples have major element contents approaching those of the undepleted mantle (*McDonough*, 1990). Their REE patterns are similar to those of the primitive mantle (Fig. 5A). Thus, spinel lherzolite xenoliths of Sangilen Plateau generally have major and trace element features that are typical of mantle peridotites that have undergone variable depletion due to partial melting.

Several models have been proposed concerning the origin of spinel-garnet clinopyroxenite xenoliths: Such rocks may be high-pressure cumulates of alkaline basalt melt, by analogy with megacryst assemblages. They could also represent inclusions of upper mantle rocks. Finally they may be regarded as cumulates, which are cogenetic with gabbroic xenoliths similar to Group IIIa in magma chambers occurring near the crust-mantle boundary.

The low Ti content in clinopyroxenes of Group II xenoliths in comparison with clinopyroxenes of the megacryst assemblage of the alkaline basalt host, represented by titanaugite, as well as the low Ti and alkali contents in the rocks suggest that Group II xenoliths are not high-pressure cumulates of alkaline basalt magma. The relatively low Mg# number, high Al and Fe contents in spinel-garnet clinopyroxenite, the low Cr content in their clinopyroxene, coupled with geothermobarometric estimations, show that they could not be magmatic cumulates within the lithospheric mantle.

Many of the major element characteristics of the spinel-garnet clinopyroxenites are similar to those of the gabbroid xenoliths. REE patterns of Group II xenoliths show similarities to the gabbroid xenoliths in relation to MREE and HREE contents. The low LREE contents may be due to the absence or minor amount of plagioclase in spinel-garnet clinopyroxenites. The pressure estimates obtained from mineral thermobarometry showed that these xenoliths were formed at pressures of 10–13 kbar. These values coincide with pressure estimates of garnet gabbroid formation conditions. Thus, the Group II xenoliths may have originated as ultramafic cumulates cognate with the garnet gabbroid (Group IIIa) close to the crust-mantle boundary. A similar origin has been suggested for lower crustal xenoliths from other areas (*Downes* et al., 2001; *Upton* et al., 1998; *Litasov* et al., 2000; *Kempton* et al., 2001).

The mineral assemblages, the mineral chemical characteristics, in particular the Al-content of pyroxenes, and thermobarometric estimates of the gabbroic xenoliths are consistent with a formation at three depth levels of crystallization of basalt melt. The deepest formations are represented by gabbroids with garnet and high-Al pyroxenes. Garnet-free gabbroids with high-Al pyroxenes are formed at intermediate depth, and gabbroids with low-Al pyroxenes are related to crystallization at shallow levels. Each rock type can contain pyroxenes and garnet with both high and low Mg# numbers, suggesting fractional crystallization within magma chambers located at different depths. The alumina content in clinopyroxenes of the Bashkymugur intrusion intruded by dikes of alkaline basalt, is 1–3 wt.%. The pressure during formation of the Bashkymugur gabbroids was estimated to be 3–4 kbar (*Izokh* et al., 2001). Thus both, the products of deep crystallization of basalt melts in intermediate chambers, and the fragments of rocks, crystallized at levels close to the formation depths of layered mafic intrusions occur among the gabbroid xenoliths of the Sangilen Plateau.

Most of the gabbroic xenoliths are similar in petrography, mineralogy and chemistry to rocks of the Bashkymugur intrusion. This intrusion is a large body of 20×5 kilometer size, elongated in north–south direction and composed of gabbroids and monzodiorites, intruded in two phases. The gabbroids are characterized by primary magmatic layering, composed of a cyclic alternation of plagiowebsterites, gabbronorites and anorthosites, sometimes with monzodiorites in upper parts of the cycles. The quantity of monzodiorites of the early phase is small, but their volume in the second phase greatly exceeds the volumes of layered gabbroids of the first phase. Such a volume of monzodiorites can only be obtained through the presence of a large intermediate magma chamber. *Shelepaev* et al. (2003) showed that the rocks of the

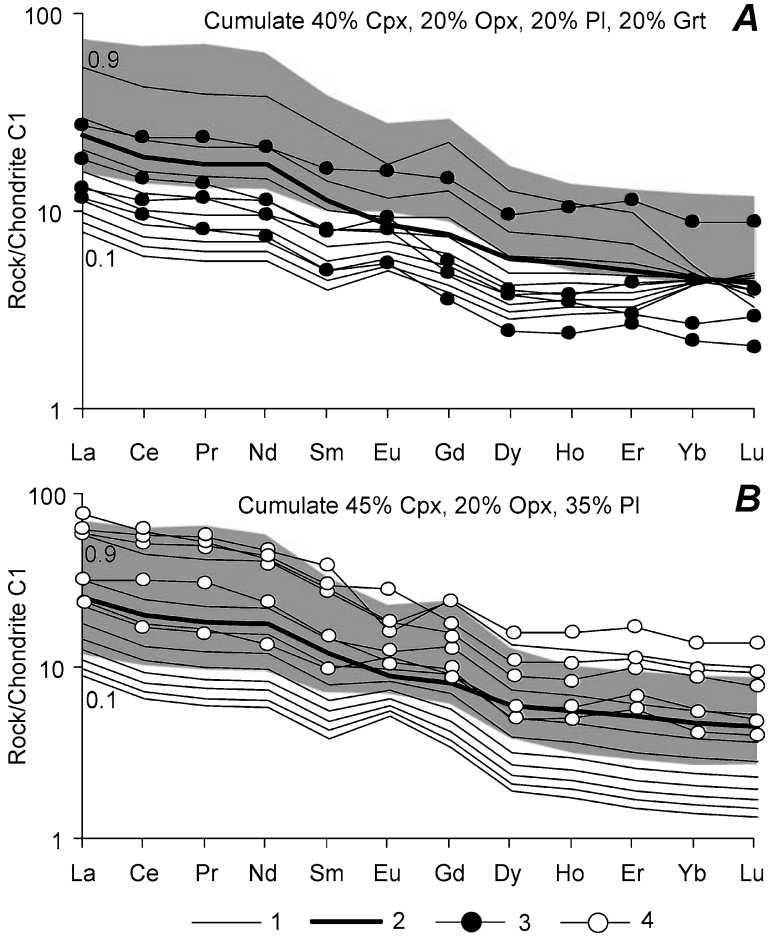

Fig. 6. Model chondrite-normalized REE patterns for crystal fractionation of clinopyroxene + orthopyroxene + plagioclase + garnet and clinopyroxene + orthopyroxene + plagioclase cumulates from melts parental to the Bushkymugur rocks (SH3); the model REE patterns are shown for varying degrees of fractionation from $F = 0.1$ to $F = 0.9$, where F is the fraction of melt remaining. 1 – model patterns; 2 – parental melt; 3 – garnet gabbroids; 4 – garnet-free gabbroids; The shaded field indicates the range of REE concetnrations in rocks from the Bushkymugur intrusion

Bashkymugur intrusion were formed from a high-alumina moderately alkaline basalt melt.

Using a simple Rayleigh fractional crystallization model and mineral/basalt partition coefficients (*McKenzie* and *O'Nions*, 1991), the REE patterns of the gabbroic xenoliths Group III can be modeled reasonably from the melt, which is parental for rocks of the Bashkymugur intrusion. A sample of olivine microgabbronorite (SH-3) was used as a compositional analogue of parental melt for the simulation of cumulate compositions. The simulation results are given in Fig. 6. For the selected parent composition the REE patterns of the Bashkymugur intrusion rocks and gabbroid xenoliths lie above the line of fractionation degrees of 0.5; this suggests considerable fractionation of the melt before crystallization of the considered rocks. The composition of gabbroic xenoliths and conducted simulations suggest the possibility of formation of gabbroic xenoliths and the Bashkymugur intrusion from the same moderately alkaline basalt melts. The occurrence of gabbroic xenoliths is a direct evidence for the existence of deep-seated chambers, in which fractionation of moderate-alkaline basaltic melt took place.

The composition of the lithosphere beneath the Sangilen Plateau

This is the first study focusing on the upper mantle composition, and the thickness and composition of the crust beneath the Sangilen Plateau. Inasmuch as the age of the host rocks is Late Ordovician, the data obtained from the xenoliths relate to composition and structural features of the lithosphere beneath the Sangilen Plateau during the Palaeozoic.

Spinel lherzolites have temperatures of equilibration ranging from 1040 to 1120 °C and equilibration pressures from 18 to 21 kbar (≈54–63 km). The results are close to the transition depth between spinel and garnet lherzolites. Based on calculated *P–T* conditions, these deep-seated xenoliths were derived from the uppermost mantle. Thus, the Ordovician lithospheric mantle beneath the Sangilen Plateau was mainly composed of spinel lherzolites.

The estimated pressure range of spinel-garnet clinopyroxenites and garnet gabbroids is 10–13 kbar (≈33–40 km). 14 kbar is the highest value reported for crustal xenoliths worldwide (*Rudnick*, 1992). Thus, the pressure estimates indicate a depth of origin for these xenoliths near the crust-mantle boundary and a crust thickness of about 40 kilometers beneath the Sangilen Plateau. *P–T* estimates and mineral compositions suggest that the garnet-free Group IIIb xenoliths were also formed under lower crustal conditions, but at a slightly shallower level than the Group IIIa garnet gabbroids. Pressure estimates indeed indicate that the Group IIIb xenoliths with high-Al pyroxenes were derived from depths of ≈24–30 km. Moreover, some Group IIIb xenoliths containing low-Al pyroxenes, originated from a level close to that of gabbroid massifs occurring in the area, i.e. in the uppermost crust of the Sangilen Plateau. This is supported by *P–T* estimations that give lower pressure values in the range of 4–7 kbar for such xenoliths, which corresponds to a depth of 12–21 kilometers. Figure 7 illustrates the inferred Early Palaeozoic crust-mantle structure of the lithosphere beneath the Sangilen Plateau, in particular it shows the location of upper mantle peridotite xenoliths and the intermediate magma chambers within the crust.

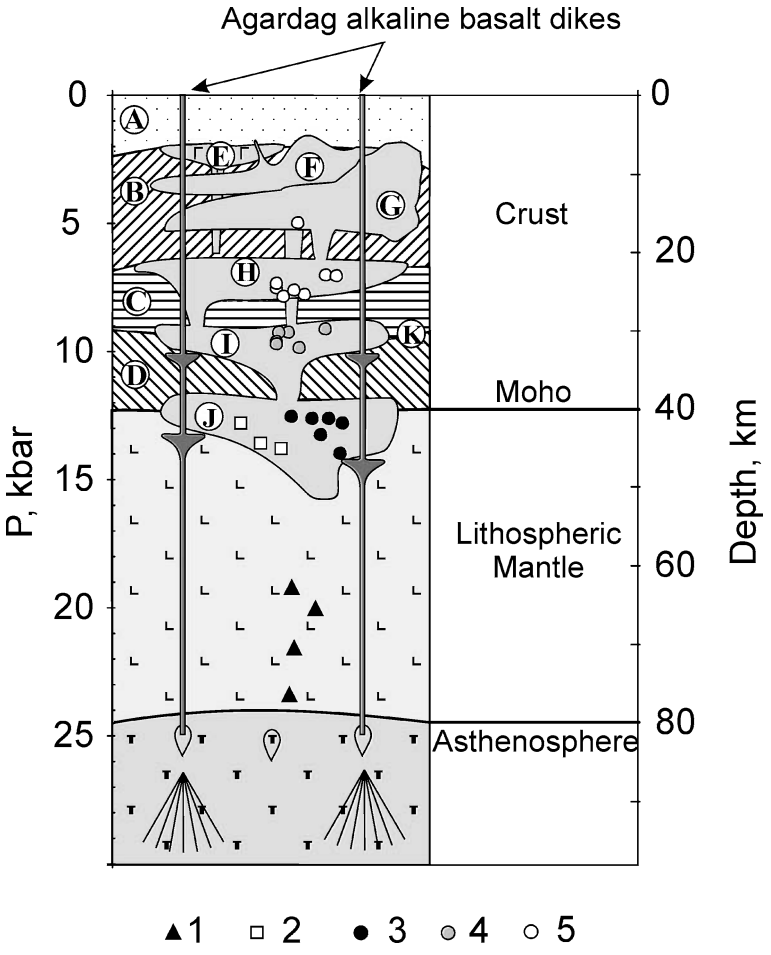

Fig. 7. Schematic representation of the crust – upper mantle structure beneath the Sangilen Plateau in Early Palaeozoic times according to data from peridotite, pyroxenite and gabbroic xenoliths. A – Cambrian volcanogenic – sedimentary rocks; B – Moren complex; C, D – lower crust; E – Pravotarlashkin intrusion; F – gabbroids of the Bushkymugur intrusion; G – monzodiorite of Bushkymugur intrusion; H, I, J – intermediate magmatic chambers; K – overlaps. 1–5 – xenoliths: 1 – spinel lherzolite, 2 – spinel-garnet clinopyroxenite, 3–5 – gabbroids: 3 – garnet, 4 – with high – Al clinopyroxenes, 5 – with low – Al clinopyroxenes

Spinel lherzolite types closely define a local paleogeotherm substantially hotter ($\sim$70–80 mW/m^2) than that of the lithospheric mantle beneath the Siberian platform (45 mW/m^2) and close to estimates of thermal flow for the Baikal rift zone (70 mW/m^2) (*Khutorskoy* and *Yarmolyuk*, 1989; *Zorin* et al., 1990). Such a hot geotherm points towards the existence of a hot plume under the Sangilen Plateau during the Ordovician, as proposed by other investigators (*Kovalenko* et al., 2004). The relatively high equilibration temperatures of garnet-spinel clinopyroxenites and gabbroids are probably also largely attributable to such a hot plume. The abundance of Ordovician high-magnesian intrusions and picrite lavas in CAOB (Kuznetsk Alatau, Mongolian Altai, Southeastern Tuva), which were formed by

high degree partial melting of the mantle (15–25%) (*Izokh* et al., 2004; *Borodina* et al., 2004), corroborate the existence of such a mantle plume during the Early Palaeozoic.

Conclusions

The spinel lherzolite xenoliths represent the uppermost lithospheric mantle beneath Sangilen Plateau and give evidence of the existence of both depleted and undepleted lithospheric mantle domains. Spinel-garnet clinopyroxenite and gabbroid xenoliths are of igneous origin and are the fragments of intrusive bodies crystallized at depth levels close to the mantle-crust boundary, as well as in the lower and upper crust. The gabbroid xenoliths are the crystallization products of melts similar in major and trace element composition to the parental magma of the Bushkymugur gabbronorite-monzodiorite intrusion. Based on mineral compositions of gabbroid xenoliths, as well as their P–T estimations, three depth levels of crystallization of moderately alkaline basaltic magma, occurring in intermediate chambers beneath Sangilen Plateau, were established for the Early Palaeozoic. Fractional crystallization taking place in each chamber stipulated for the wide compositional range of gabbroid xenoliths. The lower crust beneath the Sangilen Plateau is mainly mafic in composition and is represented by gabbroic rocks formed as cumulates from basaltic magmas. The relatively high equilibration temperatures of the mantle and lower crust xenoliths in the Agardag alkaline basalt dikes are probably attributable to a plume occurring beneath the Sangilen Plateau during the Ordovician.

Acknowledgements

The authors have benefited greatly from the comments by *H. Downes* (University of London, UK) which helped to improve the original manuscript. We are most grateful to *S. Maaløe* and anonymous reviewer for critical and constructive reviews of the manuscript. We thank *L. N. Pospelova* for the microprobe analyses. *A. D. Kireev* is thanked for XRF analyses. *L. V. Smirnova* and *G. P. Sandimirova* are thanked for ICP MS analyses. This work is supported by RFBR through grants No. 04-05-64439, 04-05-64467, 04-05-64437, 05-05-64317, research grants ''Scientific Schools'' (4933.2006.5 and 4922.2006.5) and special research grant for young scientists No. 1730.

References

Borodina EV, Egorova VV, Izokh AE (2004) Petrology of Ordovician collision-related layered peridotite-gabbro intrusions (exemplified by the Mazhalyk untrusion, Southeastern Tuva). Russian Geology and Geophysics 45: 1074–1091

Brey GP, Kohler T (1990) Geothermobarometry in four-phase lherzolites II. New thermobarometers, and practical assessment of existing thermobarometer. J Petrol 31: 1353–1378

Downes H (1993) The nature of the lower continental crust of Europe: petrological and geochemical evidence from xenoliths. Physic Earth Planetary Interior 79: 195–218

Downes H, Dupuy C (1987) Textural, isotopic and REE variation in spinel peridotite xenoliths, Massif Central, France. Earth Science Planetary Letters 82: 121–135

Downes H, Upton BGJ, Handisyde E, Thirlwall MF (2001) Geochemistry of mafic and ultramafic xenoliths from Fidra (Southern Uplands, Scotland): implications for lithospheric processes in Permo-Carboniferous times. Lithos 58: 105–124

Ellis DJ, Green DH (1979) An experimental study of the effect of Ca upon garnet-clinopyroxene Fe–Mg exchange equilibria. Contrib Mineral Petr 71: 13–22

Gasparik T (1984) Two-pyroxene thermobarometry with new experimental data in the system $CaO–MgO–Al_2O_3–SiO_2$. Contrib Mineral Petr 87: 87–97

Gibsher AS, Vladimirov AG, Vladimirov VG (2000) Geodynamics of the Early Paleozoic thrust-and-fold structure of the Sangilen, Southeastern Tuva. Doklady Earth Sciences 370: 50–53

Hammarstrom JM, Zen EA (1986) Aluminium in hornblende: an empirical igneous geobarometer. Am Mineral 71: 1297–1313

Harley SL (1984) The Solubility of alumina in orthopyroxene coexisting with garnet in $FeO–MgO–Al_2O_3–SiO_2$ and $CaO–FeO–MgO–Al_2O_3–SiO_2$. J Petrol 25: 665–694

Hollister LS, Grissom GC, Peters EK, Stowell HH, Sisson VB (1987) Confirmation of the empirical correlation of Al in hornblende with pressure of solidification of calc-alkaline plutons. Am Mineral 72: 231–239

Ilyin AV (1990) Proterozoic supercontinent, its latest Precambrian rifting, breakup, dispersal into smaller continents, and subsidence of their margins: evidence from Asia. Geology 18: 1231–1234

Ionov DA, O'Reilly SY, Griffin WL (1998) A geotherm and lithospheric section for Central Mongolia (Tariat region). Mantle Dynamics and Plate Interaction in East Asia. In: *Flower MFJ, Chung SL, Lo CH, Lee TY* (eds), Geodyn Ser 27 Am Geophys Union, Washington, DC, pp 127–153

Irving AJ (1974) Geochemical and high pressure experimental studies of garnet pyroxenite and pyroxene granulite xenoliths from the Delegate basaltic pipes, Australia. J Petrol 15: 1–40

Izokh AE, Agafonov LV, Borisenko AS, Tolstykh ND, Slutzker EM, Babich VV, Lobanov KV, Goverdovskiy VA (2004) Kuznetsk Alatau-Altai platinum-bearing belt in west Altai-Sayan fold region (Russia-West Mingolia). In: *Khanchuk AI* et al. (ed), Metallogeny of the Pasific northwest: tectonics, magmatism and metallogeny of active continental margins. Proceedings of the interim IAGOD conference, pp 350–352

Izokh AE, Polyakov GV, Mal'kovets VG, Shelepaev RA, Travin AV, Litasov YD, Gibsher AA (2001) The Late Ordovician age of camptonites from the Agardag Complex of southeastern Tuva as an indicator of the plume-related magmatism during collision processes. Doklady Earth Sciences 379: 511–514

Kempton PD, Downes H, Neymark LA, Wartho JA, Zartman RE, Sharkov EV (2001) Garnet granulite xenoliths from the northern Baltic Shield – the underplated lower crust of a Palaeoproterozoic Large Igneous Province. J Petrol 42: 731–764

Kempton PD, Downes H, Sharkov EV, Vetrin VR, Ionov DA, Carswell DA, Beard A (1995) Petrology and geochemistry of xenoliths from the Baltic Shield: evidence for partial melting and metasomatism in the lower crust beneath an Archean Terrane. Lithos 36: 157–184

Khutorskoy MD, Yarmolyuk VV (1989) Thermal and magmatic evolution of the lithosphere of Mongolia. Int Geol Rev 31: 1084–1096

Kovalenko VI, Yarmolyuk VV, Kovach VP, Kotov AB, Kozakov IK, Salnikova EB, Larin AM (2004) Isotope provinces, mechanisms of generation and sources of the continental crust in the Central Asian mobile belt: geological and isotopic evidence. J Asian Earth Sci 23: 605–627

Kozakov IK, Salnikova EB, Bibikova EV, Kirnozova TI, Kotov AB, Kovach VP (1999) Polychronous evolution of the Paleozoic granitoid magmatism in the Tuva-Mongolia Massif: U–Pb geochronological data. Petrology 7: 592–601

Leake BE, Wooley AR, Alps CES, Birch WD, Gilbert MC, Grice JD, Hawthorne FC, Kato A, Kish HJ, Krivovichev VG, Linthout K, Laird K, Mandarino JA, Maresch WV, Nickel EH, Rock NMS, Schumacher JC, Smith DC, Stephenson NCN, Ungaretti L, Whittaker EJW, Youzhi G (1997) Nomenclature of amphiboles: report of the Subcommittee on amphiboles of the International Mineralogical Association, Commision on new minerals and mineral names. Can Mineral 35: 219–246

Litasov KD, Foley SF, Litasov YD (2000) Magmatic modification and metasomatism of the subcontinental mantle beneath the Vitim volcanic field (East Siberia): evidence from trace element data on pyroxenite and peridotite xenoliths from Miocene picrobasalt. Lithos 54: 83–114

Loock G, Stosch HG, Seck HA (1990) Granulite facies lower crustal xenoliths from the Eifel, West Germany: petrological and geochemical aspects. Contrib Mineral Petr 105: 25–41

Maaløe S, Aoki K (1977) The major element composition of the upper mantle estimated from the composition of lherzolite. Contrib Mineral Petr 63: 161–173

McDonough WF (1990) Constraints on the composition of the continental lithospheric mantle. Earth Science Planetary Letters 101: 1–18

McKenzie D, O'Nions RK (1991) Partial melt distributions from inversion of rare earth element concentrations. J Petrol 32: 1021–1091

Mercier J-CC (1980) Single-pyroxene thermobarometry. Tectonophysics 70: 1–37

Morimoto N (1988) Nomenclature of pyroxenes (International Mineralogical Association). Am Mineral 73: 1123–1133

Newton RC, Perkins D III (1982) Thermodynamic calibration of geobarometers based on the assemblages garnet-plagioclase-orthopyroxene (clinopyroxene)-quartz. Am Mineral 67: 203–222

Nickel KG, Green DH (1985) Empirical geothermometry for garnet peridotites and implication for two-pyroxene thermometry. Earth Planetary Science Letters 73: 158–170

Nimis P (1999) Clinopyroxene geobarometry of magmatic rocks. Part 2. Structural geobarometers for basic to acid, tholeiitic and mildly alkaline magmatic systems. Contrib Mineral Petr 135: 62–74

O'Reilly SY, Jackson I, Bezant C (1990) Equilibration temperatures and elastic wave velocities for upper mantle rocks from eastern Australia: implication for interpretation of seismological models. Tectonophysics 185: 67–82

Powell R (1985) Regression diagnostics and robust regression in geothermometer/geobarometer calibration: the garnet-clinopyroxene geothermometer revised. J Metamorph Geol 3: 231–243

Rudnick RL (1992) Xenoliths – samples of the lower continental crust. In: *Fountain DM, Arculus R, Kay RW* (eds), Continental Lower Crust. Elsevier, New York, pp 269–316

Rudnick RL, Jackson I (1995) Measured and calculated elastic wave speeds in partially equilibrated mafic granulite xenoliths: implication for the properties of an underplated lower continental crust. J Geophys Res 100: 10211–10218

Salnikova EB, Kozakov IK, Kotov AB, Kroner A, Todt W, Nutman A, Yakovleva SZ, Kovach VP (2001) Age of Palaeozoic granites and metamorphism in the Tuvino-Mongolian massif of the central Asian mobile belt: loss of a Precambrian microcontinent. Precambrian Res 110: 143–164

Schmidt MW (1991) Amphibole composition as a function of buffer assemblage and pressure: an experimental approach, EOS, Transactions, American Geophysical Union. AGU 1991 Fall Meeting 72: 547

Sen G, Jones R (1989) Experimental equilibration of multicomposition pyroxenes in spinel peridotite field: Implication for practical thermometers and possible barometers. J Geophys Res 94: 17871–17880

Shelepaev R, Izokh A, Egorova V (2003) Geochemistry of collisional gabbroids of Western Sangilen (Southeastern Tuva, Russia). Abstract to the EGS-AGU-EUG Join Assembly. Geophysical Research Abstracts 5: 00550

Stosch HG, Ionov DA, Puchtel IS, Galer SJG, Sharpouri A (1995) Lower crystal xenoliths from Mongolia and their bearing on the nature of the deep dust beneath central Asia. Lithos 36: 227–242

Sun S-S, McDonough WF (1989) Chemical and isotopic systematics of oceanic basalts: implications for mantle compositions and processes. In: *Saunders AD, Norry MJ* (eds), Magmatism in Oceanic Basins. Geology Society Special Public 42: 313–345

Upton BGJ, Aspen P, Rex DC, Melcher F, Kinny P (1998) Lower crustal and possible shallow mantle samples from beneath the Hebrides – evidence from a xenolithic dyke at Gribun, western Mull. J Geol Society 155: 813–828

Vladimirov AG, Gibsher AS, Izokh AE, Rudnev SN (1999) Early Paleozoic granitoid batholiths of Central Asia: abundance, sources and geodynamic formation conditions. Doklady Earth Sciences 369: 1268–1271

Webb SA, Wood BJ (1986) Spinel-pyroxene-garnet relationship and their dependence on Cr/Al ratio. Contrib Mineral Petr 92: 471–480

Zonenshain LP, Kuzmin MI, Natapov LM (1990) Geology of the USSR: a plate-tectonic synthesis. AGU Geodynamics Series 21

Zorin YuA, Novoselova MR, Turutanov EK, Kozhevnikov VM (1990) Structure of the lithosphere of the Mongolian-Siberian Mountainous Province. J Geodyn 11: 327–342

Authors' addresses: *V. V. Egorova* (corresponding author, e-mail: verae@uiggm.nsc.ru), *N. I. Volkova* (e-mail: nvolkova@uiggm.nsc.ru), *R. A. Shelepaev* (e-mail: rshel@uiggm.nsc.ru), *A. E. Izokh*, Institute of Geology and Mineralogy, Russian Academy of Sciences, Koptyug pr., 3, Novosibirsk 630090, Russia